Stochastic Model-Predictive Control for Lane Change Decision of Automated Driving Vehicles

Jongsang Suh, Heungseok Chae, and Kyongsu Yi, *Member, IEEE*

***Abstract*—This paper describes lane change motion planning with a combination of probabilistic and deterministic prediction for automated driving under complex driving circumstances. The autonomous lane change should arrive safely at the destination. The subject vehicle needs to perceive and predict the behaviors of other vehicles with sensors. From the information of other vehicles, a collision probability is defined using a reachable set of uncertainty propagation. In addition, the lane change risk is monitored using predicted time-to-collision and safety distance to guarantee safety in lane change behavior. A safe driving envelope is defined as constraints based on the combinatorial prediction (probabilistic and deterministic) of the behavior of surrounding vehicles. To obtain the desired steering angle and longitudinal acceleration to maintain the automated driving vehicle under constraints, a stochastic model-predictive control problem is formulated. The proposed model has been evaluated by performing lane change simulations in MATLAB/Simulink, while considering the effect of combination prediction. Also, the proposed algorithm has been implemented on a test vehicle. The simulation and test results show that the proposed algorithm can handle complicated lane change scenarios, while guaranteeing safety.**

***Index Terms*—Automated driving control, lane change decision, real-time implementation, stochastic model predictive control, vehicle test.**

I. Introduction

ACCORDING to an accident report from Volvo, human error is the major reason for nearly 90% of accidents [1]. Lane change maneuver is the cause of various severe highway accidents, due to inaccurate estimation of the surrounding traffic, or illegal maneuver. The advanced driver assistant system (ADAS), or automated driving, is regarded as a solution to reduce human errors. Currently, automated driving is widely considered as the mainstream of automakers, since it offers increased safety and comfortability. Many vehicle manufacturers aim to commercialize self-driving cars by 2020, and spur the intelligent vehicle research necessary for its realization. Many kinds of researches have attempted to integrate individual active safety systems for the improvement of automated driving systems to enhance safety and achieve zero fatalities [2], [3].

Cost function based approaches highway motion planning for automated driving systems was proposed to implement robust freeway driving [4]. Overtaking data of human driver was analyzed and patterned of longitudinal and lateral acceleration as trapezoidal and sinusoidal shape, respectively [5]. An object-oriented Bayesian network approach was introduced for the detection of lane change maneuvers [6]. A neural network based approach for considering uncertainties was introduced to predict the maneuver trajectory as human behaviors [7], and fuzzy logic to solve modeling lane change decision-making problems [8]. Lane change trajectory is generated according to the vehicle states, surrounding vehicles, and road information. Previous researches suggest lane change trajectory generation methods that should consider estimated status of neighboring vehicles for safe lane change [9], [10]. Lane change trajectories, such as circular, cosine, polynomial and trapezoidal acceleration profile, have been investigated and compared [11], [12].

Since lane change for driver is required to predict not only other traffic, but also the subject vehicle, a MPC approach has been shown to be an attractive method for the automated driving control [13], [14]. The MPC method uses a dynamic vehicle model to predict the future states, and determines an optimal control sequence for every step, to minimize a predefined performance index satisfying the control and state constraints [15]. In [16], Falcone *et al*. present an active steering controller to follow the desired trajectory using MPC, while satisfying constraints. In order to compensate for the effect of model uncertainty and disturbance, a robust MPC that uses a linear feedback control law based on the analysis of robust invariant sets was introduced, and used to design an automated vehicle control algorithm [17]. However, the robust MPC approaches may be too conservative because of worst-case consideration [18]. In [19], Georg *et al*. present the scenario model predictive control for lane change assistance system. However, the scenario MPC may be too affected by scenario generation that need on any generic model-based or data-based method. The stochastic MPC in [20] shows the chance-constraints optimization problem for automated driving vehicles in uncertain environments.

The study focuses on designing an autonomous control algorithm that manages potentially dangerous lane change situations while satisfying control performance on model uncertainties and sensor disturbances. The vehicle motion for lane changing or keeping is defined in consideration of stochastic prediction of near future states of the surrounding circumstances, to enhance safety given the potential behavior of surrounding vehicles. A safe driving envelope is defined to guarantee safe driving for the

Manuscript received February 14, 2017; revised July 10, 2017 and September 27, 2017; accepted February 5, 2018. Date of publication February 12, 2018; date of current version June 18, 2018. This work was supported by the Institute of Advanced Machines and Design, Seoul National University, by the Brain Korea 21 program (F14SN02D1310), by the Korea Ministry of Land, Infrastructure and Transport, and by the Korea Agency for Infrastructure Technology Advancement (16PTSI-C054118-08). The review of this paper was coordinated by Dr. A. Chatterjee. *(Corresponding author: Kyongsu Yi.)*

J. Suh is with the University of California, Berkeley, CA 94720 USA (e-mail: azuresky@snu.ac.kr).

H. Chae and K. Yi are with Seoul National University, Seoul 151-744, South Korea (e-mail: gmdtjr@snu.ac.kr; kyi@snu.ac.kr).

Color versions of one or more of the figures in this paper are available online at http://ieeexplore.ieee.org.

Digital Object Identifier 10.1109/TVT.2018.2804891

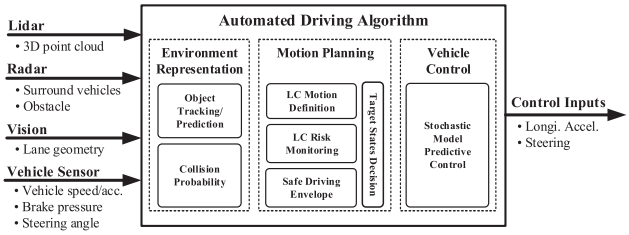

Fig. 1. Overall architecture of the proposed automated driving system.

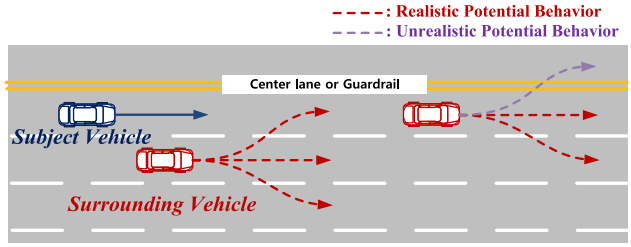

Fig. 2. Possible behavior of surrounding vehicles with the consideration of general traffic rules.

automated driving vehicle. In order to change lanes in complex surrounding traffic situations, target state decision can manage lane change motion of automated driving. Then, a SMPC problem is formulated to determine the desired control input, while maintaining the subject vehicle within the safe driving envelope.

In this paper, unlike previous studies that use deterministic prediction [13], [14], [16], [19], the lane change decision algorithm using deterministic and probabilistic prediction of other traffic participants' states to enhance robustness is proposed. The idea of using probabilistic prediction was originally proposed by Suh and Yi for the lane change [21]. The robust MPC in Ref [21] is replaced the stochastic MPC in this paper, which helps to solve the problem of too conservative robust MPC. In addition, the human driver data based lane change motion is analyzed for comfortability. The proposed algorithm determines overall process of lane change itself under spatial constraints safely, such as on/off ramps or existence of preceding vehicle. Previous researches manage too simple scenario in on/off ramps or only predict other traffic in deterministically. [22], [23]. Also, the proposed algorithm is implemented in the test vehicle on real road. Previous studies have validated the algorithm using SMPC for vehicle control in only simulation [19], [20]. Fig. 1 shows an overall architecture of the proposed automated driving system. The proposed algorithm consists of the following three steps: an environment representation, a motion planning, and a vehicle control.

This paper is structured as follows: Section II derives the environment representation model, which consists of object tracking and prediction, and *CP*. Section III defines the vehicle model. Section IV describes the motion planning design with a safe driving envelope to determine lane change or maintain motion. Section V presents a SMPC based lower level controller. Section VI presents the simulation and test results for evaluation of the performance of the proposed algorithm. Section VII summarizes the contribution of this research, and introduces future works.

II. Environment Representation Model

Precise and comprehensive environment perception is essential for safe and comfortable automated driving in complex traffic situations [24]. The sensor setup was already modified available in our test vehicles as follows: A multilayer laser scanner was added to monitor static obstacles with increased precision. For lane detection, an additional monocular vision system was mounted on the windshield.

The environment representation consists of two modules: object tracking/prediction, and *CP*. The object tracking and prediction module computes the uncertainty propagation for traffic participants. A Markov chain is used to approximate the probabilistic processes of each traffic participant. It is assumed that drivers may maintain the current vehicle behavior, such as lane keeping or changing and keep the appropriate lane in the finite prediction horizon. A simple path following model and a state predictor interact with each other during one cycle of the prediction process.

A. Object Tracking and Prediction

One of the common approaches to predict the future states of the traffic situations surrounding subject vehicles is a deterministic prediction that assumes that other vehicles surrounding the subject vehicle maintain their current movement during a finite time-horizon. However, since this approach ignores the probability of all possible movements of surrounding vehicles, it could not properly recognize unexpected driving situations. Therefore, deterministic prediction causes incorrect interpretation of the current driving situation.

In order to compensate the shortcomings of deterministic prediction of the behaviors of surrounding vehicles, the probability behaviors of surrounding vehicles are predicted, and the risk behaviors among the possible behaviors of other vehicles surrounding the subject vehicle are considered, to determine the safe driving envelope.

To predict reasonable and realistic behaviors of surrounding vehicles, the interaction between vehicles and restrictions on the surrounding vehicles' maneuver due to road geometry should be considered [25]. Thus, in predicting the possible behaviors of surrounding vehicles, it is assumed that surrounding vehicles are driven with the consideration of the presence of other vehicles, and interactive motions with other vehicles, respectively. This means that for collision avoidance, the minimum safety distance between surrounding vehicles should be kept.

Also, it is assumed that drivers of the surrounding vehicles maneuver their vehicles with consideration of the road geometry. This means that the speed of the surrounding vehicles should be adapted to the road geometry and road condition.

Moreover, it is assumed that drivers of the surrounding vehicles obey general traffic rules [24]. If one of the surrounding vehicles changes lane, then that vehicle is assumed to keep to the proper lane in the far-off future. Furthermore, Fig. 2 shows that violation of the centerline of surrounding vehicles is prohibited.

In predicting reasonable ranges of the future states of surrounding vehicles, driving data is collected on the real road to analyze the probabilistic movement characteristics of the other vehicles. For the implementation of these assumptions, a path-following model is designed while interacting with a vehicle state predictor during one cycle of the prediction process. The details of the path-following model are in [26]. In the vehicle state predictor, the vehicle's probable position and its error covariance over a finite time horizon are predicted by an

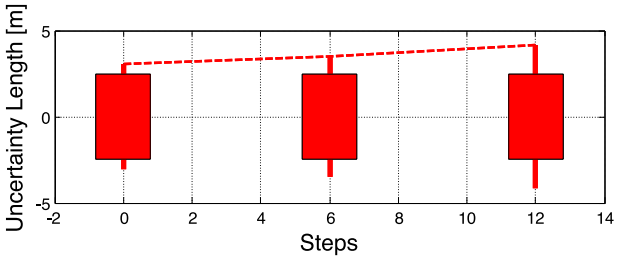

Fig. 3. Uncertainty propagation of the target vehicle.

Extended Kalman Filter, using the desired yaw rate obtained by the path-following model as the virtual measurement [26].

Fig. 3 shows the simulation results for uncertainty propagation of the target vehicle. The red square describes vehicle shape. When the prediction step grows, the uncertainty gets larger. The uncertainty at the current step is 0.68 m; after six steps, it is 1.22 m; and after 12 steps, it is 1.95 m.

B. Collision Probability

At the beginning of the collision probability estimation, a given number N state vectors is randomly generated based on probability density function from the prediction algorithm. Since a trade-off between computational burden and collision probability approximation accuracy, the N has to be chosen by a designer.

The study scrutinizes that the vehicle shapes of the target vehicles intersect that of the subject vehicle at each predicted time step for every possible pair of the target vehicle and the subject vehicle. Fig. 4 summarizes and presents the concepts of probabilistic collision risk. In this research, the prediction time for collision probability is 5 seconds.

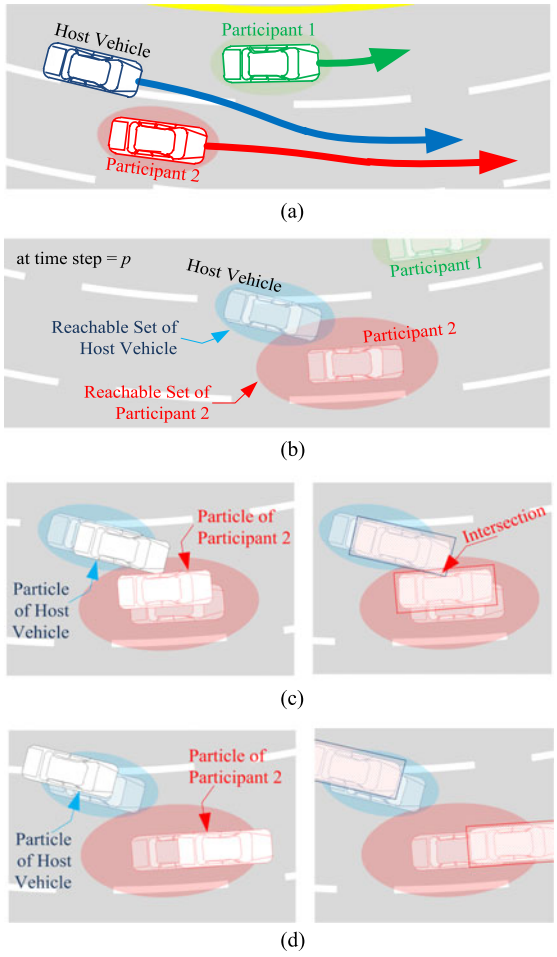

Fig. 4. Procedure and concept of the approximation of collision probability. (a) Environment description based on sensor fusion: road geometry, the subject vehicle's current motion, and multitraffic participant. (b) Visualized example of a prediction of multitraffic pose and their covariance at a predictive time step. Reachable sets of each participant are in stochastic distribution. (c) A collision case example of the generated *N* particles and two vehicle-body-shaped polygons. The intersection is defined between two polygons. (d) A noncollision case example of the generated *N* particles and two vehicle-body-shaped polygons.

III. Vehicle Model

A vehicle dynamics model should be derived to obtain the desired control inputs with the SMPC approach. In this research, a linear parameter varying (LPV) model of the vehicle dynamics is designed from the nonlinear vehicle model. Nonlinear differential equations are used to describe the behavior of the vehicle in the Frenet frame [27],

$$\dot{v}_x = v_y\gamma + a_x \tag{1a}$$

$$\dot{v}_y = -v_x\gamma + \frac{1}{m}\left(2F_{yf} + 2F_{yr}\right) \tag{1b}$$

$$\dot{\gamma} = \frac{1}{I_z}\left(2l_f F_{yf} - 2l_r F_{yr}\right) \tag{1c}$$

$$\dot{e}_\psi = \gamma - \kappa\dot{s} \tag{1d}$$

$$\dot{e}_y = v_x \sin\left(e_\psi\right) + v_y \cos(e_\psi) \tag{1e}$$

$$\dot{s} = \frac{1}{1-\kappa e_y}\left(v_x \cos\left(e_\psi\right) - v_y \sin\left(e_\psi\right)\right) \tag{1f}$$

$$F_{y*} = k_* C_* \alpha_*, \quad {}^* \in \{f, r\} \tag{1g}$$

$$\alpha_f = \delta_f - \frac{v_y + l_f\gamma}{v_x} \tag{1h}$$

$$\alpha_r = -\frac{v_y - l_r\gamma}{v_x} \tag{1i}$$

where, l_f and l_r denote the distance from the center of gravity of vehicle to the front and rear axles, respectively; m and I_z denote the vehicle mass and yaw inertia, respectively; e_ψ is the orientation error of the vehicle with respect to the road; e_y denotes the lateral offset with respect to the centerline of the lane; κ is the curvature of the road from camera sensor; s denotes the longitudinal position of the vehicle with curvature along the road; F_{yf} and F_{yr} are lateral forces of front axle and those of rear axle in the body frame, respectively; k_* is the cornering stiffness adjustment coefficients to reflect a tire saturation characteristic; C_* denotes the lateral tire cornering stiffness; α_* denotes the lateral tire slip angle; and l_f and l_r denote the distances from the vehicle's center of gravity to the front and rear axles, respectively. Fig. 5 depicts a diagram of the vehicle model.

The nonlinear vehicle model can be compactly defined as follows:

$$\dot{x}(t) = f\left(x(t)\ u(t)\ d(t)\right) \tag{2}$$

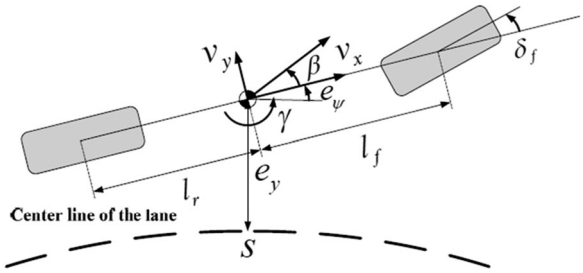

Fig. 5. Diagram of the dynamics model.

where, $x = [\,v_x\ v_y\ \gamma\ e_\psi\ e_y\ s\,]^T$, $u = [\,\delta_f\ a_x\,]^T$, and $d = \kappa$ are state, input and disturbance vector, respectively. δ_f denotes steering angle and a_x denotes longitudinal acceleration. Normally, force or pressure actuated to the vehicle wheels by applying voltage for wheel motors or for hydraulic-pressure model. However, in this paper, the ADAS is utilized for vehicle control. δ_f is lateral control input utilizing the lane keeping assistance system (LKAS) and a_x is longitudinal control input utilizing the adaptive cruise controller (ACC).

However, the critical barrier to implementation in real-time is the computational load to solve the nonlinear predictive problem. To deal with this issue, a linearized tire model with Taylor expansion with several assumptions is applied to obtain an LPV model of the vehicle dynamics. The details of vehicle model are in [28].

The modified LPV model is discretized as,

$$x_{k+1} = \mathbf{A}_{l,k}x_k + \mathbf{B}_{l,k}u_k + \mathbf{D}_{l,k}w_k \tag{3}$$

where, $w_k \sim N(0, \Sigma_w)$. The disturbance covariance, Σ_w, is estimated in Section V.

IV. Motion Planning Algorithm

When driving on the road, a lane change is necessary for several reasons, such as planning to take an upcoming exit way, or the preceding vehicle driving slower than a speed limit. The automated driving vehicle adjusts its lane keeping or changing motion to follow the traffic situations. Furthermore, to stay in a safe driving area is important to avoid collision with other vehicles or obstacles. Just as human drivers consider the surrounding environment and predict a period of the future states of the subject and other vehicles, object prediction information is used in Section II to plan the subject vehicle's motion. To develop a highly automated driving system, the appropriate vehicle behavior and the safe driving envelope should be simultaneously determined with the present and near future states of the traffic situations. The reference position calculation considers that the subject vehicle changes its lane safely in complex lane change situations. To guarantee safety of reference positions, the *TTC* and *CP* are adopted.

A. Lane Change Motion Definition

A lane change is a very important part of vehicle behavior. Since the control strategies for lane keeping and changing for automated driving vehicles are different, determining vehicle motion is critical to set the control strategy.

In order to obtain the lateral motion for lane change, previous research has standardized lateral acceleration for lane change maneuver as a sinusoidal shape [5]. However, regarding ride quality, the sinusoidal shape has excessive acceleration jerk value. In this paper, a hyperbolic tangent path is suggested for low acceleration jerk.

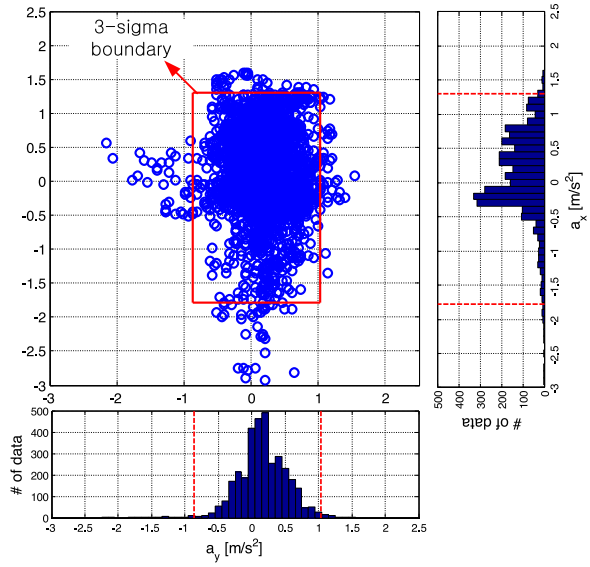

Fig. 6. Data of 22-human-driver-based acceleration analysis.

The information to obtain proper lateral acceleration is the road width, lane change process time, and acceleration limit. Fortunately, the road width can be measured using information of the vision sensor. The acceleration limit can be analyzed based on the data using a test vehicle. The total number of measured data sets is 318 for 22 drivers. Data is measured in urban roads and motorways. Fig. 6 shows individual driver data based acceleration analysis results.

Fig. 6 shows that human drivers use lateral acceleration of less than 1 m/s^2 in most situations. It is reasonable to set the maximum lateral acceleration as 1 m/s^2.

Then, define the hyperbolic tangent path as follows:

$$e_{y,\mathrm{ref}}(t) = C_1 \cdot \tan h\,(C_2 \cdot t + C_3) + C_4 + e_{y,0} + L_p \tag{4}$$

where,

$$C_1 = \frac{\pm W_{\mathrm{road}} - e_{y,0}}{2} \qquad C_2 = \sqrt{\frac{a_{y,\mathrm{lim}}}{a_{y,0} \cdot C_1}}$$

$$C_4 = \frac{\pm W_{\mathrm{road}} - e_{y,0}}{2} \qquad C_3 = -\frac{t_{LC}}{2}C_2$$

$$t_{LC} = \frac{2}{C_2}\tan h^{-1}\left\{\frac{W_{\mathrm{road}} - C_4 - e_{y,0}}{C_1}\right\}$$

where, subscript 0 denotes current information; L_p denotes preview distance; and *t* denotes time parameter; lateral acceleration limit magnitude denotes $a_{y,\mathrm{lim}}$; W_{road} denotes the road width; $a_{y,0}$ is the original maximum magnitude of lateral acceleration; t_{LC} denotes lane change process time; C_* is a constant value C_1 through C_4 which are calculated via simple calculations with two assumptions:

Assumption 1: The lateral velocity for the lateral lane change motion is zero.

Assumption 2: The lateral motion does not rely on the longitudinal velocity as shown in Fig 7.

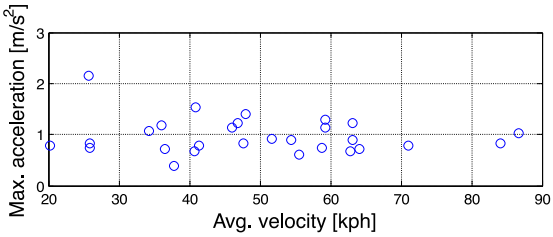

Fig 7. Human-driver-data-based maximum lateral acceleration for average velocity.

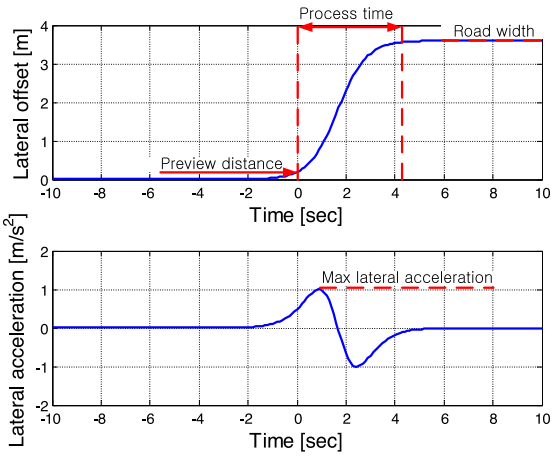

Fig. 8. Hyperbolic-tangent-based lateral offset and lateral acceleration.

Fig. 8 shows the hyperbolic tangent based path and acceleration that reflect the parameters.

B. Lane Change Risk Monitoring

The lane change risk constraints should be calculated to determine the lane change direction. For example, if after the subject vehicle crosses the lane, a fast rear-side vehicle appears, a hazardous situation would occur. The lane change risk monitoring investigates the safety of the subject vehicle to judge risk during the lane change process. The lane change risk is monitored so that the process time is larger than the *TTC* between the subject vehicle and other target vehicles or distance between the subject and another vehicle that is less than a safe distance. If one or more of these conditions are violated, the lane change risk monitoring prevents the subject vehicle from changing lane. In addition, the probabilistically predicted information of the subject and other vehicles can be obtained in Section III. Therefore, even if risk constraint uses *TTC*, and the safe distance and these indices are calculated in every predicted step. This means that the lane change risk monitoring uses probabilistic information to judge the risk situation.

The lane change risk constraints can be written as,

$$|c_k| > c_{\text{safe}}$$

$$c_{\text{safe}} = c_{th} + \max_k \left(\sigma_{n,k}\right) \tag{5a}$$

$$TTC_{n,k} \geq \left(t_{LC} - k \cdot t_{\text{samp}}\right), \quad k = 1, \ldots, N_p \tag{5b}$$

where, c denotes clearance; c_{safe} denotes minimum safety distance; c_{th} denotes the minimum acceptable distance to avoid a collision; σ denotes uncertainties of the position of other vehicles; n denotes target vehicle number; k denotes prediction step; N_p denotes maximum prediction step; and t_{samp} denotes sampling time.

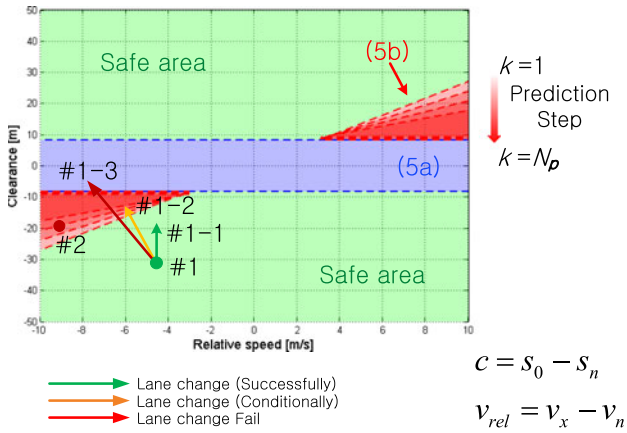

Fig. 9. Risk monitoring for the lane change procedure. The blue area and the red area indicate (5a) and (5b), respectively.

Fig. 9 shows the diagram of lane change risk constraints. c denotes the clearance with the subject vehicle and the target vehicle, s_0 is the longitudinal position of the subject vehicle, s_n is the longitudinal position of the target vehicle, and v_{rel} denotes relative velocity, v_x is the velocity of the subject vehicle, and v_n is the velocity of the target vehicle.

From (5a) and (5b), there are two constraints for monitoring lane change risk. The blue and red areas in Fig. 9 are described by (5a) and (5b), respectively. In particular, the constraints for (5b) have several areas that indicate consideration of the prediction steps of the limitations. It is evident that the red constraint decreases its area as the prediction step proceeds.

Assume that the subject vehicle wants to change lane. However, there is a side-rear vehicle that is faster than the subject vehicle. In this situation, the subject vehicle could be in danger. From this assumption, three detailed scenarios can be deduced.

First, #1 means that the vehicle is in the lane change safe area. It can be predicted that the subject vehicle can change lane successfully. If there is enough space and a similar relative speed, the subject vehicle can change its lane as #1-1, which means that the subject vehicle is still in a safe area and changes lane successfully. As the subject vehicle moves to the next lane, the required lane change time reduces. Accordingly, the lane change process can still be in progress, whether or not the distance is larger than the constraint for (5a). However, assume that the side-rear vehicle has accelerated more, but not by much. Then #1 draws a trajectory like #1-2. In this case, the risk monitoring algorithm investigates whether the vehicle behavior will violate the *TTC* constraints considering the prediction time. If the side-rear vehicle accelerates much more, then #1 is expected to move to #1-3. This means that clearance between the subject vehicle and side-rear vehicle is less than the (5a) constraint. Therefore, the lane change risk algorithm prevents the subject vehicle from changing lane. If the subject vehicle tries to change lane in #2, the lane change risk also avoids lane change.

C. Safe Driving Envelope Definition

After deciding to change lane, the subject vehicle needs constraints to guarantee safety in various situations, such as remaining in its lane, maintaining enough distance from other traffic

participants, or changing lane. In the lane keeping situation, the subject vehicle should keep a safe distance, while preparing for a vehicle that cuts in. In the lane change situation, the subject vehicle needs to change lane without any collisions.

For the decision of the safe driving envelope to improve safety, a potentially hazardous situation should be considered. Various dangerous situations among the future behaviors of the surrounding vehicles can be roughly classified into three types. First, if the preceding vehicle in the originating lane of the subject vehicle unexpectedly decelerates, then the collision probability between the preceding vehicle and the subject vehicle increases. Second, if the side approaching vehicle in the adjacent lane accelerates during a lane change maneuver of the subject vehicle, then collision between the approaching vehicle and the subject vehicle could be expected. Third, there could be a potential risk of collision due to a vehicle sudden cutting-in from the adjacent lane. Therefore, to improve safety to avoid these three situations, determining the safe driving envelope considers not only current states of the surrounding environment of the subject vehicle, but also these potentially dangerous behaviors of the surrounding vehicles over a finite prediction horizon.

In lane keeping, the driving envelope is determined to keep to the originating lane and maintain safety. Let us assume that the lateral clearance that is expected at a certain prediction timestep between the subject vehicle and the surrounding vehicle is larger than a predefined threshold value. Then the safe driving envelope for the lateral boundary is determined as the road width of the originating lane. Otherwise, if the adjacent vehicle approaches the originating lane of the subject vehicle, the safe driving envelope narrows its width using uncertainties and states of the predicted surrounding vehicles. If the preceding vehicle is slower than the subject vehicle, the longitudinal safe driving envelope is defined using the present and predicted position of the preceding vehicle with safety distance. However, if there is no preceding vehicle, or the preceding vehicle is faster than the subject vehicle, then only the vehicle speed is considered to set the safe driving envelope. Therefore, the environmental envelope is determined to remain in the originating lane, while evading the hazardous approaching adjacent vehicle.

The safe driving envelope is determined to change lane to the proper direction for lane change. Similar to the safe driving envelope for lane keeping, the current and predicted states of surrounding vehicles are considered. However, since the drivable area should be secured to the next lane for safe lane change, the safe driving envelope lateral expands its area into the next lane. The longitudinal safe driving envelope considers a nearer vehicle between the preceding or the side-front vehicle to determine a drivable area. The preceding vehicle and the side-front vehicle should be regarded as one vehicle, since when the subject vehicle changes lane, the subject vehicle is simultaneously located in both lanes. As the side-rear vehicles are already considered to guarantee safety, the safe driving envelope is defined using the current and predicted states of surround vehicles. The safe driving envelope is presented in detail in [21].

Consequently, the lateral and longitudinal safe driving envelope can be defined as,

$$g_k^T \cdot x_k \leq h_k, \quad k = 1, \ldots, N_p \tag{6}$$

where

$$g_k = \begin{bmatrix} 0 & 0 & 0 & 0 & 1 & 0 \\ 0 & 0 & 0 & 0 & 0 & 1 \\ 0 & 0 & 0 & 0 & -1 & 0 \\ 0 & 0 & 0 & 0 & 0 & -1 \end{bmatrix}^T$$

$$h_k = \begin{bmatrix} \alpha W_{\text{road}} \\ \min\left(s_{\text{side-front}},\ s_{\text{preceding}}\right) - \tau_h v_x \\ \beta W_{\text{road}} \\ -s_{\text{side-rear}} - \tau_h v_x \end{bmatrix}$$

$$(\alpha, \beta) = \begin{cases} \left(\frac{3}{2}, \frac{1}{2}\right) & \text{if left lane change} \\ \left(\frac{1}{2}, \frac{3}{2}\right) & \text{elseif right lane change} \\ \left(\frac{1}{2}, \frac{1}{2}\right) & \text{otherwise} \end{cases}$$

where, the subscript *upper* and *lower* are the upper boundary and lower boundary position of the subject vehicle. The s with subscript *preceding, side-front*, and *side-rear* are a longitudinal position of preceding vehicle, side-front vehicle, and side-rear vehicle, respectively. If there is no front vehicle to consider, they are replaced by a predefined threshold value. In a similar way, if there is no side-rear vehicle, the threshold value is used to define the longitudinal position constraints. τ_h is the headway time, which is the mean value of the time gap for the driving data in the following situations [29].

D. Target State Decision

When lane change is necessary, the appropriate lateral motions are necessary. However, it may occur that the subject vehicle should conduct lane change in some situations such as merge, split, or intersection. Then the automated driving vehicle is necessary to adjust its longitudinal position and velocity to change lane to match the traffic flow and reach a safe area of the next lane.

For lane keeping, since the subject vehicle needs to remain in the lateral constraints of safe driving envelope, the lateral position is determined by the center of the originating lane. The longitudinal position and velocity are defined to follow the desired speed. However, if the preceding vehicle that is slower than the subject vehicle exists, the desired speed is set as the velocity of the preceding vehicle.

For lane change, as long as safety is guaranteed, the velocity maintains the desired speed. However, if risk is predicted in the near future, the longitudinal position and velocity of the subject vehicle are determined to follow the traffic flow of the target lane, the destination of the subject vehicle. Also, the subject vehicle should stay in the safe area between the side-rear and side-front vehicles.

When the subject vehicle keeps its lane, it needs to maintain sufficient clearance between the subject vehicle and the preceding vehicle. The desired clearance is regarded as a boundary problem, because if the clearance from the subject vehicle to the preceding vehicle is too far to consider, the subject vehicle does not need to accelerate to adjust for this clearance. However, if the clearance is too close so as to present a danger, the subject vehicle should slow down its speed to be safe. The desired

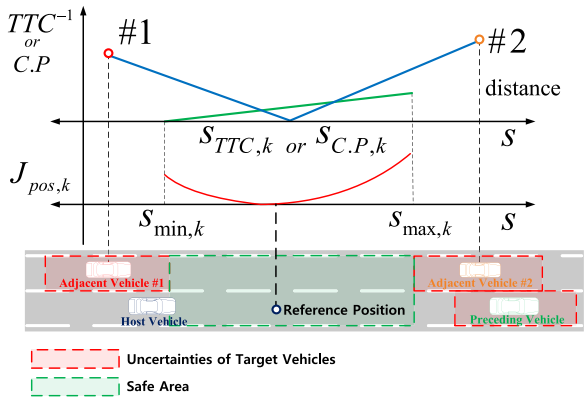

Fig. 10. Desired longitudinal position calculation at the kth step.

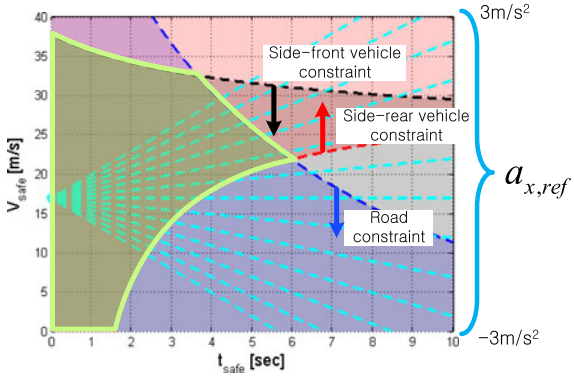

Fig. 11. Constraints of a limited situation.

clearance is defined as follows:

$$c_{\text{des}} = \tau_h \cdot v_x + c_{\text{safe}} \tag{7}$$

Assume that the subject vehicle should change, but for several reasons it is hard to change lane. Then, the subject vehicle should accelerate or decelerate to find a safe area to change lane safely. In general, difficulties in lane change situations for human drivers arise when traffic flow varies between the originating lane of the subject vehicle, and the adjacent lane. In this case, the driver accelerates the subject vehicle to change lane or adjusts speed to that of the adjacent vehicle, and determines longitudinal position guaranteed safety. Similarly, the decision algorithm sets the speed of the target vehicle that has the highest *CP* as the desired speed to follow. Though the safe area is defined as distance, MPC problem needs a certain point as a reference. A simple optimization problem is used to obtain the reference point, because the optimization method is easily adjusted with a predefined simple cost function. The optimization problem is formulated to obtain the safest longitudinal position in terms of *TTC* and *CP* as follows:

$$\min_{s_{LC,k}} \quad J_{\text{pos},k} = \begin{bmatrix} l_1(s_{LC,k} - s_{TTC,k})^2 + l_2\,|s_{LC,k} - s_{\text{dist},k}| \\ + l_3(s_{LC,k} - s_{CP,k})^2 \end{bmatrix} \tag{8a}$$

$$\text{s.t.} \quad s_k < s_{\max,k} \tag{8b}$$

$$s_k > s_{\min,k}$$

$$k = 1, \ldots, N_p \tag{8c}$$

where, s_{TTC}, s_{CP}, and s_{dist} denote positions that are calculated by *TTC* and *CP*, distance from the subject vehicle, and *CP* of vehicles, respectively. l_i denotes the i-th weighting factor. $s_{\max}$ and $s_{\min}$ are the maximum and minimum boundaries of longitudinal position defined by the longitudinal constraint of the safe driving envelope. The reference s_{LC} is calculated at every step to minimize this cost function. Fig. 10 shows the desired longitudinal position calculation at k-th step.

Fig. 10 shows that the desired longitudinal reference position is calculated from the linear proportion of the surrounding vehicles' inverse TTC and CP as the blue line. The distance from the host vehicle to the desired longitudinal position is penalized to prevent excessive acceleration described as green line. The longitudinal target position is determined by these considerations inside the minimum and maximum boundaries that are defined as the safe driving envelope. After the host vehicle reaches the safe area, the subject vehicle starts to change lanes.

However, if there are constraints of time or distance, such as a merging section or slow preceding vehicle, the subject vehicle needs to change lane in a limited time. Furthermore, if the adjacent vehicles exist in the side-lane, the safe area is defined as constraints. In this constrained situation, a reference velocity should be obtained to reach the desired longitudinal reference position from (8) quickly.

For straightforward and fast planning for lane change, the assumption is as follows:

Assumption 3: When the vehicle changes lane, the vehicle accelerates with constant longitudinal acceleration.

In order to obtain the desired reference velocity, v_{safe}, three constraints are defined as follows:

$$\frac{v_x + v_{\text{safe}}}{2} t_{\text{safe}} - v_{\text{side-rear}} t_{\text{safe}} \geq c_{\text{safe}} + c_{0,\text{side-rear}} \tag{9a}$$

$$\frac{v_x + v_{\text{safe}}}{2} t_{\text{safe}} + v_{\text{safe}} t_{LC} \leq c_{\text{end}} \tag{9b}$$

$$\frac{v_x + v_{\text{safe}}}{2} t_{\text{safe}} + v_{\text{safe}} t_{LC} - v_{\text{side-front}} \left(t_{\text{safe}} + t_{LC}\right) \leq -c_{\text{safe}} + c_{0,\text{side-front}} \tag{9c}$$

where, t_{safe} denotes the acceleration completion time; c_0 denotes initial clearance; c_{end} denotes distance from the host vehicle to road end considering the marginal area. The desired reference velocity is calculated under these constraints to avoid collision.

If there is no side-rear vehicle, (9a) is always satisfied. If neither end road situation exist, like merging section or slow preceding vehicle, (9b) is also satisfied. Similarly, when the side-front does not exist, (9c) does not need to be considered.

Fig. 11 presents the simulation results. Side-front and side-rear vehicles are faster than the host vehicle. The initial speeds of the side-front and side-rear vehicle are both 80 kph, and the initial speed of the host vehicle is 60 kph. Distance to the end of the road is 150 m.

The grey area is the side-front vehicle constraint, the red area is the side-rear vehicle constraint, and the blue area is the road constraint. The area of the overlap of all three constraints is shown in green. Cyan lines represent constant acceleration candidates that have bounds -3 m/s^2 through 3 m/s^2.

When the host vehicle enters the road, positive acceleration is primarily considered. If multiple solutions can be obtained by constraints, the proposed algorithm chooses minimum

acceleration among the possible candidates. However, if there is no solution with positive acceleration, the proposed algorithm calculates the solution using negative acceleration candidates.

To change lane in various situations, references to lateral and longitudinal states are calculated over the finite prediction horizon to keep or change the lane. The lateral and longitudinal references are operated in SMPC over the finite prediction horizon. The references can be rewritten as follows:

$$v_{x,\mathrm{ref}} = \begin{cases} v_{flow} & \text{if nonconstrained LC} \\ v_x & \text{otherwise} \end{cases} \tag{10a}$$

$$s_{\mathrm{ref}}, k = \begin{cases} s_{LC,k} & \text{if nonconstrained LC} \\ s_{ref,k-1} & \text{otherwise} \end{cases} \tag{10b}$$

V. Stochastic MPC-Based Vehicle Control

In this section, the disturbance analysis and MPC problem formulation are introduced. The vehicle dynamic model utilized for control is introduced, and its uncertainties are considered. The uncertainties include measurement errors of vehicle and exterior sensors, and model mismatch to define disturbance covariance. In order to formulate MPC with chance-constraints, tightened constraints are applied to calculate the optimization problem possible. The stability of this closed-loop system has been proved in other papers [30], [31]. This optimization problem is solved at each step, and the first terms of the optimal control sequences are applied to the system. A solver FORCES which is designed to be utilizable in MATLAB is used [32].

A. Disturbance Analysis

To formulate the SMPC, the bounded additive disturbance of the model should be defined. Experimental data is used to identify the bounded disturbance *w*. The one-step state prediction using the system model is compared with the current measured data [33]. The system model is discretized with a sampling time of 100 ms.

$$e_k = x_{k+1} - \mathbf{A}_{l,k} x_k - \mathbf{B}_{l,k} u_k \tag{11}$$

Using the results of disturbances, the disturbance covariance is derived as,

$$\Sigma_w = \mathrm{diag}\left(0.120,\ 0.043,\ 0.009,\ 0.003,\ 0.018,\ 0.002\right) \tag{12}$$

B. SMPC-Based Desired Control Input Decision

The study presents the SMPC problem which is used to decide the desired control inputs for control performance. The SMPC problem is formulated using the vehicle dynamics model and safe driving envelope constraints. The SMPC is solved to determine a sequence of control inputs that are applied to the system. The solving process of the optimization problem repeated at each time step is formulated as follows:

TABLE I
Parameters of the MPC Problem

Parameters	Value
$\mathbf{Q}$	$\mathrm{diag}(0.2, 0.5, 0.1, 1, 0.2, 0.05)$
$\mathbf{R}$	$\mathrm{diag}(10, 5)$
$u_{\max}$	$[30,\ 3]^{\mathrm{T}}$
$u_{\min}$	$[-30,\ -5]^{\mathrm{T}}$

$$\min \quad \sum_{k=0}^{N_p-1} \mathbb{E}\left(\|x_{t+k+1,t} - x_{ref,k+1}\|_{\mathbf{Q}}^2 + \|u_{t+k,t}\|_{\mathbf{R}}^2 \right) \tag{13a}$$

$$\text{s.t.} \quad x_{t+k+1,t} = \mathbf{A}_{l,k} x_{t+k,t} + \mathbf{B}_{l,k} u_{t+k,t} + \mathbf{D}_k w_k \tag{13b}$$

$$\Pr\left(g_{k+1}^T x_{k+1} \le h_{k+1}\right) \ge 1 - \varepsilon_k \tag{13c}$$

$$u_{k,t} \le u_{\max} \tag{13d}$$

$$u_{k,t} \ge u_{\min} \tag{13e}$$

$$x_{t,t} = x(t) \tag{13f}$$

$$(k = 0, \ldots, N_{p-1})$$

where, $\mathbf{Q}$ and $\mathbf{R}$ denote weighting matrices; t is the current time instant; $x_{t+k,t}$ is the predicted subject vehicle state at time $t+k$ derived by applying the control sequence u_t to the vehicle model (13b) with initial condition (13f); (13c) is a chance constraint to be satisfied with a specified probability $0 \le \varepsilon \le 0.5$; ε denotes the tunable risk parameter; and (13d) and (13e) are control input constraints, $u_{\max} = [\delta_{f,\lim},\ \ a_{x,\max}]^T$ and $u_{\min} = [-\delta_{f,\lim},\ \ a_{x,\min}]^T$.

Table I shows the parameters of MPC problems.

Using the closed-loop paradigm [30], the chance constraints (13c) can be rewritten as,

$$g_{k,i}^T z_{k,i} \le h_{k,i} - \gamma_{k,i}, \quad i = 1, \ldots, l \tag{14}$$

where, z_k is defined as nominal state variables, $x_k = z_k + e_k$; l denotes row number of matrix g_k^T; γ_k is tightened parameter which is defined as,

$$\gamma_{k,i} = \sqrt{2 g_{k,i}^T \Sigma_k g_{k,i}} \mathrm{erf}^{-1}\left(1 - 2\varepsilon_i\right) \tag{15}$$

where, erf^{-1} is the inverse error function.

VI. Evaluation Results

The proposed algorithm for automated driving vehicle was evaluated via computer simulations and real vehicle test. The computer simulation was conducted using MATLAB/ Simulink and Carsim, and the test vehicle was constructed using close-to-market sensors, as mentioned in Section II.

A. Robustness Evaluation for Combinatorial Prediction

In order to show the effectiveness of the proposed algorithm using combination of probabilistic and deterministic prediction, simulation results of the control algorithm based on SMPC using deterministic prediction of the surrounding vehicle are

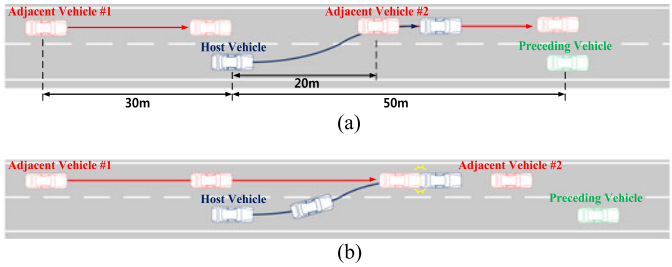

Fig. 12. Simulation scenarios of unexpected traffic. (a) Start to change lane. (b) Risk prediction during lane change.

compared with those of the proposed algorithm. The primary features of the control algorithm based on SMPC using deterministic prediction can be represented as follows:

Remark 1: The environmental envelope defined using deterministic prediction is defined without respect to the possible behavior of the surrounding vehicle.

Remark 2: The target vehicle for the control of longitudinal acceleration is generated by integrating the current states of the preceding vehicle in the originating lane, and those of the vehicle in the adjacent lane.

Since an automated driving control algorithm should operate in a wide operating region, the performance of the proposed algorithm should be verified in various driving situations. In this paper, comparison of combinatorial and only deterministic results is conducted via computer simulation.

In order to compare the decision performance, the simulation scenario is set so that the risk prediction is difficult. In other words, after the host vehicle judges present risk, and determines to change lane, the other vehicles suddenly change their motion. Fig. 12 shows the simulation scenario is designed to reproduce the risky highway situation.

In this situation, the initial velocities of adjacent vehicles are set to 80 kph, and those of the host vehicle and preceding vehicle are configured to 60 kph. The host vehicle starts to accelerate until it judges lane change to be safe. However, the adjacent vehicle #1 accelerates to prevent lane change of the host vehicle. The initial clearance between the host vehicle and the adjacent vehicle #1 is 30 m, and between the host vehicle and the adjacent vehicle #2 is 20 m. Also, the initial clearance between the host vehicle and the preceding vehicle is 50 m. Road friction is 0.95.

Simulation studies were repeated 11 times to compare control algorithms, which are combinatorial and deterministic predictions. Each simulation has different acceleration magnitudes of the adjacent vehicle #1 0 to 2 m/s^2 with interval 0.2 m/s^2.

Fig. 13 presents the simulation results. Fig. 13(a) shows the difference between vehicle trajectory using probability prediction, and that using deterministic prediction. Depending on the acceleration of the subject vehicle #1, the automated driving algorithm using deterministic prediction cannot successfully change lane. Fig. 13(b) describes the longitudinal velocity of the host vehicle. At first, the host vehicle accelerates similarly in both predictions, but the automated driving vehicle using combinatorial prediction maintains its speed. Comparing the results of Fig. 13(a) and (b), lane change juncture using the combinatorial method is determined a few seconds later. This means that using combinatorial prediction, the host vehicle secures the distance between the host vehicle and other vehicles farther than

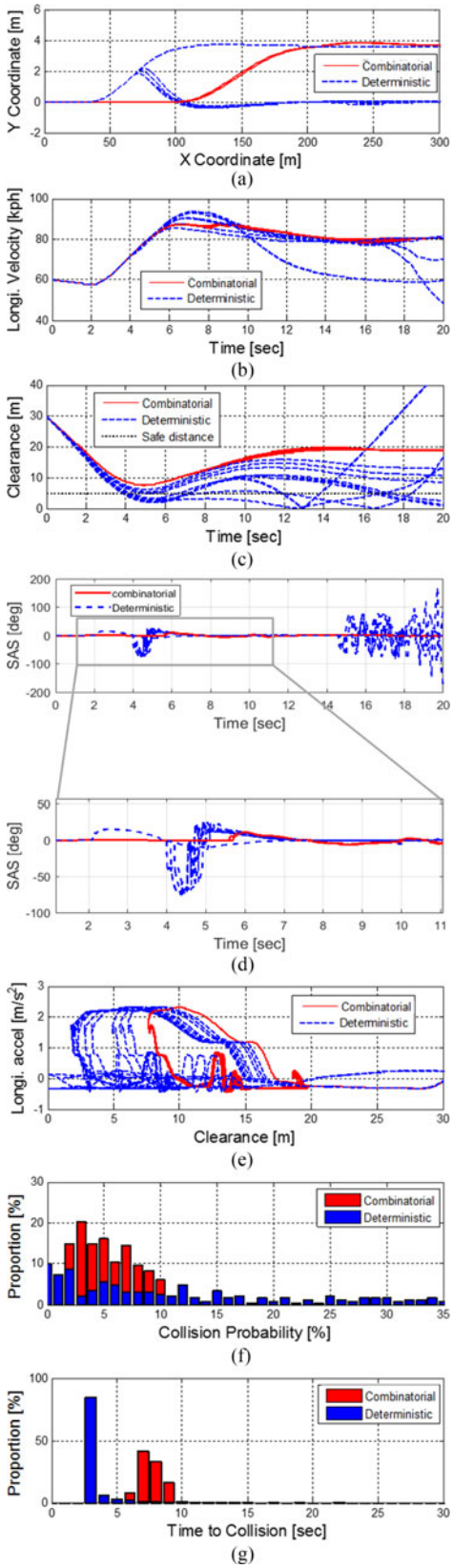

Fig. 13. Comparison of the performance results between combinatorial and deterministic prediction. (a) Vehicle trajectory. (b) Longitudinal velocity. (c) Clearance between the subject vehicle and adjacent vehicle. (d) Steering angle. (e) Longitudinal acceleration and clearance. (f) Collision probability. (g) Time to collision.

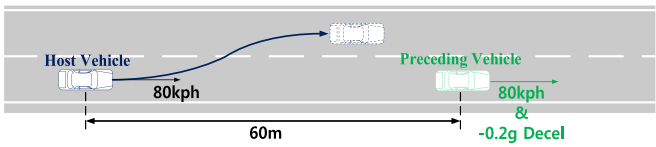

Fig. 14. Simulation scenarios of unexpected lane change situation.

by using deterministic prediction. Fig. 13(c) shows that when the deterministic prediction is used, the clearance between the host vehicle and adjacent vehicle #1 violates safe distance. In particular, using combinatorial prediction, the clearance of the host vehicle has robust performance when the motion of other traffic changes. Fig. 13(d) shows control input, steering angle. The combinatorial method for decision making has very robust performance while the algorithm using only deterministic goes unstable. Fig. 13(e) shows that clearance between the host vehicle and adjacent vehicle #1 is kept very similar. This means that the proposed algorithm has robust performance. In other words, an algorithm using deterministic prediction does not have reproducibility and robustness. To show the effectiveness of using probability prediction for safe lane change, Fig. 13(f) and (g) plot risk indices, collision probability, and *TTC*. The average value of collision probability distribution using combinatorial prediction is smaller than that using deterministic prediction. To express it differently, the mean value of *TTC* data using combinatorial prediction is larger than that using deterministic prediction. This means that combinatorial prediction is much safer than deterministic prediction.

B. Robustness Evaluation for Road Friction

In order to evaluate the proposed algorithm on various road conditions, such as road friction, the simulation studies have been conducted in high and low mu road situations. The simulation scenario is set as the unexpected lane change situation. The preceding vehicle decelerates as 0.2 g value, and the host vehicle changes lane to avoid collision. Fig. 14 shows the simulation scenario briefly.

Simulation studies were repeated 3 times to compare control algorithms in different road conditions. Each simulation has different road friction magnitudes as 0.2, 0.6, 0.9.

Fig. 15 presents the simulation results. Fig. 15(a) shows that vehicle trajectories with various road friction have almost same path to change lane. It means that the proposed lane change controller is robust for road frictions. Comparing the results of Fig. 15(b)–(d), since the controller uses longitudinal and lateral acceleration about less than 1 m/s^2, all lane change results such as longitudinal velocity, longitudinal acceleration, and lateral acceleration are similar. Fig. 15(e) shows control input, steering angle. The controller doesn't need to high lateral acceleration value to change lane, so the control input also almost same in various road conditions. In other words, the proposed algorithm is robust for various road conditions.

C. Test Results

In order to evaluate the proposed algorithm on a real test vehicle, a Hyundai-Kia Motors K7 was used as a test vehicle platform. Fig. 16 shows the test vehicle configuration. In order to measure the lateral offset, heading angle, and road curvature,

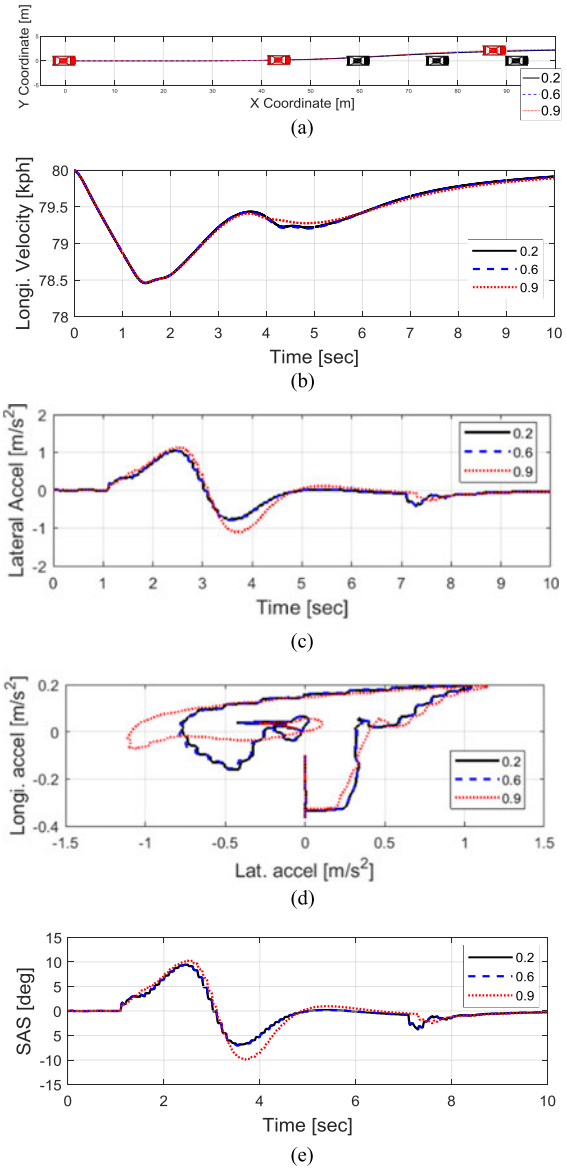

Fig. 15. Comparison of the performance results in various road friction situations. (a) Vehicle trajectory. (b) Longitudinal velocity. (c) Lateral acceleration. (d) G-G diagram. (e) Steering angle.

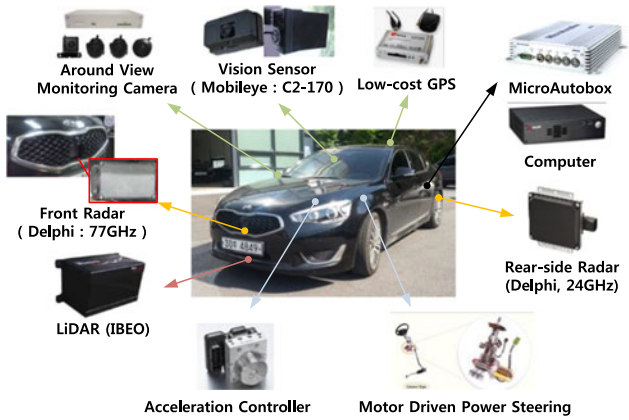

Fig. 16. Test vehicle configuration.

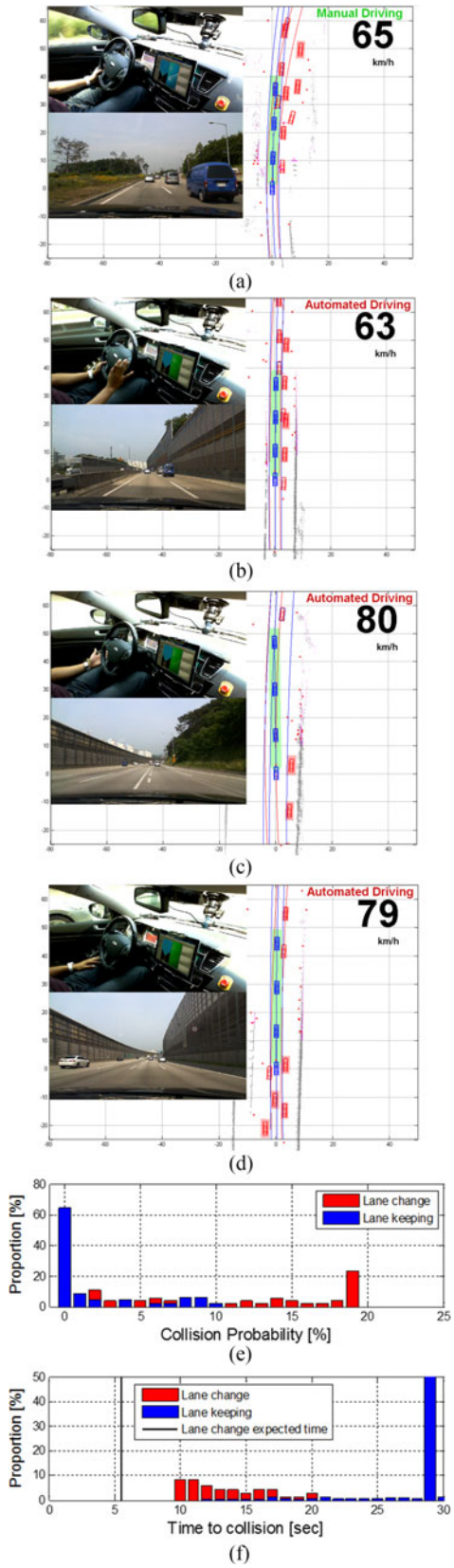

Fig. 17. Vehicle test results. (a) Human driver drives at entering section of expressway ($t = 3.3$ s). (b) The proposed algorithm takes over control authority from the human driver ($t = 10.8$ s). (c) The automated driving vehicle accelerates up to traffic flow of expressway and changes lane ($t = 32.5$ s). (d) The lane change is completed ($t = 41.9$ s). (e) Collision probability. (f) Time to collision.

a Mobileye camera system was equipped on the test vehicle. The proposed algorithm was implemented in MicroAutobox II, which is used for real-time application. Delphi radars were equipped on the test vehicle to perceive surrounding environments. An IBEO laser scanner was equipped on the test vehicle to detect static obstacles. The hardware components mentioned above communicate through a CAN bus. The computational time is about 200 ms.

Vehicle tests were conducted for several times at the on-ramp section of Yeongdong Expressway. The test vehicle drove the given route fully autonomously, without driver manipulation. The automated driving vehicle needed to consider other traffic participants, such as preceding vehicles and adjacent vehicles, and detect guardrails, while the subject vehicle ran at high speed.

The proposed automated driving algorithm showed satisfactory control performance, and Fig. 17 shows the test results. The figure shows that the host vehicle drives through a junction section with static obstacles, and preceding and adjacent vehicles. Comparison of the center paths between raw data (solid red line) and estimated data (blue solid line) of vision is given. Control input sequences from SMPC solver are depicted as a blue vehicle, which follows a center path well. The blue and red boxes depict reachable sets using uncertainty propagation. The green area means the safe driving envelope.

Fig. 17(a) shows a human driver driving at an exit section of the junction with other vehicles and both side static obstacles. It is a normal driving situation to follow the preceding vehicle. In Fig. 17(b), the proposed algorithm can take over control authority from the human driver when the driver pushes an automation button. Then the host vehicle accelerates to join the expressway, which has faster traffic flow. After reaching the traffic flow of expressway, the host vehicle maintains its speed. Fig. 17(c) shows that the proposed algorithm makes the vehicle change lane when safety is secured. The vehicle smoothly changes lane, and maintains a safe driving envelope. After the host vehicle successfully changes lane, Fig. 17(d) shows that it keeps its lane with following the traffic flow of its lane. To verify the safety performance of the proposed algorithm, collision probabilities and *TTC* were analyzed. The vehicle status are divided into two, lane keeping and lane change. Fig. 17(e) shows the histogram of the collision probability. This figure shows the proposed algorithm safely determines lane change procedure, and maintains collision probability that is lower than a certain level. In a similar way, Fig. 17(f) in particular shows time to collision results that are larger than the lane change expected time. This means that the host vehicle keeps its safety clearance from other vehicles and enough time for changing lane.

VII. Conclusion

A probabilistic and deterministic prediction based lane change motion planning and control algorithm for automated driving was developed, and the performance of the proposed algorithm was evaluated via computer simulation and test vehicle. To deal with the potential risk of the lane change situation, the current states and possible risk behaviors of the surrounding environment during a finite time horizon were simultaneously considered to determine lane keeping and change motion, and to maintain a safe driving envelope with risk monitoring. The control architecture based on a SMPC approach was used to calculate the desired steering angle and longitudinal acceleration with probabilistic constraints from uncertainties and disturbances.

Automated driving with the proposed algorithm shows smooth and safe driving behavior with safety in collision-risk road traffic situations, such as lane keeping with following a preceding vehicle, lane change in a multi-vehicle environment, and so on. In particular, the combinatorial prediction based automated driving control algorithm shows safer performance than the deterministic prediction. It was demonstrated that the proposed algorithm could operate on the test vehicle.

In the future, evaluations in more various situations should be conducted to verify the reliability of the proposed algorithm. Also, human driver data analysis based lane change decision is needed using machine learning, such as a Gaussian mixture model and Gaussian mixture regression.

REFERENCES

[1] Volvo Trucks, "European accident research and safety report," 2013. [Online]. Available: http://www.volvotrucks.com/SiteCollectionDocuments/VTC/Corporate/Values/ART%20Report%202013_150dpi.pdf

[2] R. Bishop, "A survey of intelligent vehicle applications worldwide," in *Proc. IEEE Intell. Veh. Symp.*, Dearborn, MI, USA, 2000, pp. 25–30.

[3] A. Eskandarian, *Handbook of Intelligent Vehicles*. London, U.K.: Springer, 2012.

[4] J. Wei, J. Dolan, and B. Litkouhi, "A prediction- and cost function-based algorithm for robust autonomous freeway driving," in *Proc. IEEE Intell. Veh. Symp.*, 2010, pp. 512–517.

[5] L. Wan, P. Raksincharoensak, K. Maeda, and M. Nagai, "Lane change behavior modeling for autonomous vehicles based on surroundings recognition," *Int. J. Autom. Eng.*, vol. 2, no. 2, pp. 7–12, 2011.

[6] D. Kasper *et al.*, "Object-oriented Bayesian networks for detection of lane change maneuvers," *IEEE Intell. Transp. Syst. Mag.*, vol. 4, no. 3, pp. 19–31, Fall 2012.

[7] R. S. Tomar, S. Verma, and G. S. Tomar, "Prediction of lane change trajectories through neural network," in *Proc. Int. Conf. Comput. Intell. Commun. Netw.*, 2010, pp. 249–253.

[8] E. Naranjo, C. Gonzalez, R. Garcia, and T. de Pedro, "Lane-change fuzzy control in autonomous vehicles for the overtaking maneuver," *IEEE Trans. Intell. Transp. Syst.*, vol. 9, no. 3, pp. 438–450, Sep. 2008.

[9] G. Usman and F. Kunwar, "Autonomous vehicle overtaking - an online solution," in *Proc. IEEE Int. Conf. Autom. Logist.*, 2009, pp. 596–601.

[10] A. Goswami, "Trajectory generation for lane-change maneuver of autonomous vehicles," Ph.D. dissertation, Dept. Elect. Comput. Eng., Purdue Univ., West Lafayette, IN, USA, 2015.

[11] W. Chee and M. Tomizuka, "Vehicle lane change maneuver in automated highway systems," Dept. Mech. Eng., Univ. California, Berkeley, CA, USA, PATH Res. Rep. MOU 89, 1994.

[12] M. Suzuki and Y. Furukawa, "Steering avoidance support system by DYC combined with collision mitigation brake system," in *Proc. Int. Symp. Future Active Safety Technol. Toward Zero Traffic Accidents*, Tokyo, Japan, 2011.

[13] A. Gray, Y. Gao, J. Hedrick, and F. Borrelli, "Robust predictive control for semi-autonomous vehicles with an uncertain driver model," in *Proc. IEEE Intell. Veh. Symp.*, Gold Coast, QLD, Australia, 2013, pp. 208–213.

[14] S. Anderson, S. Perters, T. Pilluti, and K. Iagnemma, "An optimal control based framework for trajectory planning, threat assessment, and semi-autonomous control of passenger vehicles in hazard avoidance scenarios," *Int. J. Veh. Auton. Syst.*, vol. 8, no. 2, pp. 190–216, Apr. 2010.

[15] D. Mayne, J. Rawlings, C. Rao, and P. Scokaert, "Constrained model predictive control: Stability and optimality," *Automatica*, vol. 36, no. 6, pp. 789–814, Jun. 2000.

[16] P. Falcone, F. Borrelli, J. Asgari, H. E. Tseng, and D. Hrovat, "Predictive active steering control for autonomous vehicle systems," *IEEE Trans. Control Syst. Technol.*, vol. 15, no. 3, pp. 566–580, May 2007.

[17] D. Mayne, M. Seron, and S. Rakovic, "Robust model predictive control of constrained linear systems with bounded disturbances," *Automatica*, vol. 41, no. 2, pp. 219–224, 2005.

[18] A. Gray, Y. Gao, T. Lin, J. Hedrick, and F. Borrelli, "Stochastic predictive control for semi-autonomous vehicles with an uncertain driver model," in *Proc. 16th Int. IEEE Conf. Intell. Transp. Syst.*, 2013, pp. 2329–2334.

[19] S. Georg and F. Borrelli, "Scenario model predictive control for lane change assistance on highways," in *Proc. IEEE Intell. Veh. Symp.*, 2015, pp. 611–616.

[20] M. P. Vitus and C. J. Tomlin, "A probabilistic approach to planning and control in autonomous urban driving," in *Proc. IEEE 52nd Annu. Conf. Decision Control*, 2013, pp. 2459–2464.

[21] J. Suh, K. Yi, J. Jung, K. Lee, H. Chong, and B. Ko, "Design and evaluation of a model predictive vehicle control algorithm for automated driving using a vehicle traffic simulator," *Control Eng. Pract.*, vol. 51, pp. 92–107, Jun. 2016.

[22] J. Wei J. M. Dolan, and B. Litkouhi, "Autonomous vehicle social behavior for highway entrance ramp management," in *Proc. IEEE Intell. Veh. Symp.*, 2013, pp. 201–207.

[23] J. Wei *et al.*, "A behavioral planning framework for autonomous driving," in *Proc. IEEE Intell. Veh. Symp. Proc.*, 2014, pp. 458–464.

[24] B. Vanholme, D. Gruyer, and B. Lusetti, "Highly automated driving on highways based on legal safety," *Intell. Transp. Syst.*, vol. 14, no. 1, pp. 333–347, Mar. 2012.

[25] M. Althoff, O. Stursberg, and M. Buss, "Model-based probabilistic collision detection in autonomous driving," *IEEE Trans. Intell. Transp. Syst.*, vol. 10, no. 2, pp. 299–310, Jun. 2009.

[26] J. Wei *et al.*, "A behavioral planning framework for autonomous driving," in *Proc. IEEE Intell. Veh. Symp.*, 2014, pp. 458–464.

[27] B. Kim and K. Yi, "Probabilistic and holistic prediction of vehicle states using sensor fusion for application to integrated vehicle safety systems," *IEEE Trans. Intell. Transp. Syst.*, vol. 15, no. 5, pp. 2178–2190, Oct. 2014.

[28] A. Carvalho, Y. Gao, S. Lefevre, and F. Borrelli, "Stochastic predictive control of autonomous vehicles in uncertain environments," in *Proc. Int. Symp. Adv. Veh. Control*, 2014.

[29] S. Moon and K. Yi, "Human driving data-based design of a vehicle adaptive cruise control algorithm," *Veh. Syst. Dyn.*, vol. 46, no. 8, pp. 661–690, Jun. 2008.

[30] B. Kouvaritakis, M. Cannon, S. V. Rakovic, and Q. Cheng, "Explicit use of probabilistic distributions in linear predictive control," *Automatica*, vol. 46, no. 10, pp. 1719–1724, Oct. 2010.

[31] M. Cannon, B. Kouvaritakis, and D. Ng, "Probabilistic tubes in linear stochastic model predictive control," *Syst. Control Lett.*, vol. 58, no. 10, pp. 747–753, Oct. 2009.

[32] A. Domahidi and J. Jerez, Forces Professional., embotech GmbH, Jul. 2014. [Online]. Available: http://embotech.com/FORCES-Pro

[33] Y. Gao, A. Gray, H. E. Tseng, and F. Borrelli, "A tube-based robust nonlinear predictive control approach to semiautonomous ground vehicles," *Veh. Syst. Dyn.*, vol. 52, no. 6, pp. 802–823, Mar. 2014.

Jongsang Suh received the B.S. and Ph.D. degrees in mechanical engineering from Seoul National University, Seoul, South Korea, in 2012 and 2016, respectively. He is a Postdoctoral Researcher in mechanical engineering with the University of California, Berkeley, CA, USA. His research interests include automated driving vehicle control, robust and stochastic model-predictive control, uncertainty compensation, and torque vectoring control.

Heungseok Chae received the B.S. degree in mechanical engineering from Seoul National University, Seoul, South Korea, in 2011, where he is currently working toward the Ph.D. degree in mechanical and aerospace engineering. His research interests include automated driving vehicle control, motion planning of automated driving vehicle, autonomous lane change, and model-predictive control.

Kyongsu Yi received the B.S. and M.S. degrees in mechanical engineering from Seoul National University, Seoul, South Korea, in 1985 and 1987, respectively, and the Ph.D. degree in mechanical engineering from the University of California, Berkeley, CA, USA, in 1992.

He is a Professor at the School of Mechanical and Aerospace Engineering, Seoul National University. His research interests are control systems, driver assistant systems, and active safety systems of ground vehicles. He is a member of the Editorial Boards of the *KSME International Journal*, the *International Journal of Automotive Technology*, and the *Journal of Institute of Control, Robotics and Systems*.